JB Journals.ASM.org

Genome-Wide Analysis of the Role of Global Transcriptional Regulator GntR1 in *Corynebacterium glutamicum*

Yuya Tanaka,[a] Norihiko Takemoto,[a] Terukazu Ito,[a,b] Haruhiko Teramoto,[a] Hideaki Yukawa,[a] Masayuki Inui[a,b]

Research Institute of Innovative Technology for the Earth, Kyoto, Japan[a]; Graduate School of Biological Sciences, Nara Institute of Science and Technology, Nara, Japan[b]

The transcriptional regulator GntR1 downregulates the genes for gluconate catabolism and pentose phosphate pathway in *Corynebacterium glutamicum*. Gluconate lowers the DNA binding affinity of GntR1, which is probably the mechanism of gluconate-dependent induction of these genes. In addition, GntR1 positively regulates *ptsG*, a gene encoding a major glucose transporter, and *pck*, a gene encoding phosphoenolpyruvate carboxykinase. Here, we searched for the new target of GntR1 on a genome-wide scale by chromatin immunoprecipitation in conjunction with microarray (ChIP-chip) analysis. This analysis identified 56 *in vivo* GntR1 binding sites, of which 7 sites were previously reported. The newly identified GntR1 sites include the upstream regions of carbon metabolism genes such as *pyk*, *maeB*, *gapB*, and *icd*, encoding pyruvate kinase, malic enzyme, glyceraldehyde 3-phosphate dehydrogenase B, and isocitrate dehydrogenase, respectively. Binding of GntR1 to the promoter region of these genes was confirmed by electrophoretic mobility shift assay. The activity of the *icd*, *gapB*, and *maeB* promoters was reduced by the mutation at the GntR1 binding site, in contrast to the *pyk* promoter activity, which was increased, indicating that GntR1 is a transcriptional activator of *icd*, *gapB*, and *maeB* and is a repressor of *pyk*. Thus, it is likely that GntR1 stimulates glucose uptake by inducing the phosphoenolpyruvate (PEP):carbohydrate phosphotransferase system (PTS) gene while repressing *pyk* to increase PEP availability in the absence of gluconate. Repression of *zwf* and *gnd* may reduce the NADPH supply, which may be compensated by the induction of *maeB* and *icd*. Upregulation of *icd*, *gapB*, and *maeB* and downregulation of *pyk* by GntR1 probably support gluconeogenesis.

Corynebacterium glutamicum is a high-GC Gram-positive soil bacterium that is traditionally used for the industrial production of amino acids (1, 2). This bacterium can also be used for efficient production of lactate and succinate from sugar (3–5). Central carbon metabolism plays a pivotal role in the generation of energy for biological processes and in the supply of precursor molecules for biosynthesis of cell compounds. Therefore, the molecular basis of its regulation is of great interest for the development of new bioprocesses.

Since the genome sequence of *C. glutamicum* was determined (1, 6, 7), several transcriptional regulators of various carbon metabolism genes have been discovered, and it is likely that these regulators, such as SugR, RamB, RamA, GlxR, LldR, and GntR1 and GntR2 (GntR1/2), form a global regulatory network (8, 9). This regulatory system is distinct from the well-studied system in *Escherichia coli* or *Bacillus subtilis*. For example, the global catabolite repression mechanism mediated by *E. coli* cyclic AMP receptor protein (CRP) or *B. subtilis* CcpA has not been established in *C. glutamicum*. In contrast, *C. glutamicum* can simultaneously utilize multiple carbon sources (10, 11). Genome-wide analysis such as microarray or chromatin immunoprecipitation (ChIP)-chip analysis was conducted for the understanding of the regulatory network of these regulators. For example, ChIP-chip analysis of GlxR detected more than 200 *in vivo* binding regions in both noncoding and coding regions of the *C. glutamicum* genome (12), establishing that GlxR is a global transcriptional regulator.

GntR1/2 is responsible for the induction of gluconate utilization genes in *C. glutamicum* ATCC 13032 (13). Expression of the *gntP* and *gntK* genes is upregulated by disruption of both of the functionally redundant *gntR1* and *gntR2* genes. This result indicates that GntR1/2 represses the genes encoding gluconate permease (GntP) and gluconate kinase (GntK) as in the cases of GntR in *E. coli* and *B. subtilis*. In addition, the pentose phosphate pathway genes *tkt*, *tal*, *zwf*, *opcA*, and *devB*, which are clustered in the genome, and *gnd* are under the control of GntR1/2 (13, 14). Gluconate and glucono-δ-lactone reduce the DNA binding activity of GntR1/2 (13). Thus, it is believed that GntR1/2 senses the presence of gluconate and glucono-δ-lactone in the cell and that decreased GntR1/2 activity results in the induction of gluconate utilization genes.

A unique characteristic of *C. glutamicum* GntR1/2 is that it functions as a transcriptional activator of *ptsG* and *ptsS*, the genes that encode the phosphoenolpyruvate (PEP):carbohydrate phosphotransferase system (PTS) for uptake of glucose and sucrose, respectively (13). The dual functions of GntR1/2, repression of gluconate utilization and activation of the PTS-dependent sugar uptake, probably contribute to the simultaneous utilization of gluconate and glucose in *C. glutamicum*. Recently, it was reported that the *pck* gene, encoding phosphoenolpyruvate carboxykinase, is also transcriptionally activated by GntR1/2 (15). Microarray analysis revealed that disruption of *gntR1/2* resulted in the upregulation of 19 genes and downregulation of 26 genes (13). However, the direct binding of GntR1/2 was demonstrated in only the seven promoter regions of the above target genes (*gntK gntP*, *tkt* operon, *ptsG*, *ptsS*, *pckA*, and *gnd*). Thus, the gene list of direct targets of GntR1/2 remains unclear.

Received 16 May 2014 **Accepted** 24 June 2014

Published ahead of print 30 June 2014

Address correspondence to Masayuki Inui, mmg-lab@rite.or.jp.

Supplemental material for this article may be found at http://dx.doi.org/10.1128/JB.01860-14.

doi:10.1128/JB.01860-14

TABLE 1 Strains used in this study

Strain	Description	Reference or source
R	JCM 18229 wild-type strain	7
KT8	R Δ*gntR1*	32
TI01	R with FLAG-tagged *gntR1*	This study
YT402	R with P*icd-lacZ*	This study
YT403	R with P*icd*Δ*GntR1site-lacZ*	This study
YT362	R with P*gapB-lacZ*	This study
YT363	R with P*gapB*Δ*GntR1site-lacZ*	This study
YT406	R with P*pyk-lacZ*	This study
YT407	R with P*pyk*Δ*GntR1site-lacZ*	This study
YT384	R with P*maeB-lacZ*	This study
YT399	R with P*maeB*Δ*GntR1site1-lacZ*	This study
YT395	R with P*maeB*Δ*GntR1site2-lacZ*	This study
YT397	R with P*maeB*Δ*GntR1site1,2-lacZ*	This study

The unique characteristic of GntR1/2, i.e., that the regulon is not limited to the gluconate utilization genes, prompted us to search for the new target of GntR1 in *C. glutamicum* R, the strain in which GntR2 is not encoded by the genome and disruption of *gntR1* is enough to induce *gnd* expression (14). In this study, we searched the *in vivo* binding site of GntR1 by ChIP-chip analysis. We identified 56 binding regions, including all the seven sites previously identified as described above. Binding of GntR1 to four of the newly identified regions upstream of carbon metabolism genes, i.e., *maeB*, *gapB*, *icd*, and *pyk*, was confirmed by electrophoretic mobility shift assay (EMSA). Disruption of the GntR1 binding site reduced the activity of *maeB*, *gapB*, and *icd* promoters but enhanced that of the *pyk* promoter. These results suggest a new role for GntR1 in the coordination of utilization of different carbon sources in *C. glutamicum*.

MATERIALS AND METHODS

Media and growth conditions. *C. glutamicum* R was grown aerobically at 33°C in nutrient-rich A medium (16) supplemented with 2% (wt/vol) glucose or gluconate. Bacterial growth was monitored by determining the optical density at 610 nm (OD_{610}).

Bacterial strains. The strains used in this study are listed in Table 1. *C. glutamicum* R was used as a wild-type (WT) strain. The strains having the *icd*, *gapB*, *pyk*, or *maeB* promoter-*lacZ* fusion gene (P*icd-lacZ*, P*gapB-lacZ*, P*pyk-lacZ*, and *PmaeB-lacZ*, respectively) with or without mutation at GntR1 binding region, were constructed as described previously (17).

Construction of plasmids used in this study. Translational promoter-*lacZ* fusion vectors were constructed as follows. The promoter region and coding sequence for the initial 5 amino acids of *icd*, *gapB*, *pyk*, and *maeB* were amplified by PCR using primers EcoRV-icd–400F and EcoRV-icd-15R for *icd*, EcoRV-gapB–400F and EcoRV-gapB-15R for *gapB*, EcoRV-pyk–390F and EcoRV-pyk-15R for *pyk*, EcoRV-maeB–410F and EcoRV-maeB-15R for wild-type *maeB*, and EcoRV-maeB–410F and EcoRV-maeB-mut GntR1-site2R for the *maeB* promoter with the mutation at GntR1 binding site 2 (Table 2). The amplified fragment was digested with EcoRV and cloned into the DraI in the site of the pCRA741 reporter plasmid (16). Mutagenesis of the GntR1 binding sites was conducted as follows. The plasmid containing *icd-lacZ*, *gapB-lacZ*, *pyk-lacZ*, or *maeB-lacZ* was used as a template for inverse PCR using corresponding primer sets (Table 2). The amplified fragment was digested with BglII and self-ligated. The resultant plasmid was used to transform *C. glutamicum* R, and a recombinant cell with a kanamycin resistance marker was selected. Insertion of the promoter-*lacZ* fusion gene between *cgR_0734* and *cgR_0735* was confirmed by PCR using primers LlacZLR-4354F and Ind7insert-checkR or LlacZLR-6425R and Ind7insert-checkF.

The *gntR1-FLAG* strain (TI01) was constructed as described previously (18). First, the DNA fragment containing the *gntR1* region was amplified from the *C. glutamicum* R genome by PCR using primers NheI-2434–1500-F5 and SalI-2434–1500-R4 (Table. 2). The amplified fragment was digested with NheI and SalI and cloned into pCRA725. The resultant plasmid was used as a template for inverse PCR to add FLAG-tag (DYKDDDK) at the C terminus of *gntR1* using primer sets C_gntR_FLAG-tag_nheI and C_nheI_gnt3′_ver4. The resultant plasmids were introduced into *C. glutamicum*, and single-crossover cells were isolated by using kanamycin resistance. Isolated cells were cultivated on medium supplemented with 10% sucrose, and double-crossover cells were isolated. The gene modifications were confirmed by DNA sequencing of the PCR products around the modified region.

ChIP-chip analysis. Exponentially growing *C. glutamicum* cultures (35 ml) in A medium with 2% glucose were treated with formaldehyde (at a final concentration of 1%) and incubated for 15 min at room temperature. The cross-linking was quenched by addition of glycine (at a final concentration of 125 mM), and the culture was incubated for 5 min at room temperature. Cells were then collected by centrifugation, washed twice with Tris-buffered saline (20 mM Tris-HCl [pH 7.5], 150 mM NaCl), and stored at −80°C. Pellets were resuspended in 0.5 ml FLAG buffer (20 mM Tris-HCl [pH 8.0], 200 mM KCl, 5 mM $MgCl_2$, 10% glycerol, 0.1% SDS) containing protease inhibitor cocktail (Roche Antiprotease Mini). The cell suspension was transferred to a 15-ml tube containing ~300 mg of 0.1-mm Zirconia/Silika beads (Bio Spec). Cell disruption and genomic DNA shearing were conducted using Bioruptor UCD-250 (Cosmo Bio) under the following conditions: 10 cycles of 5 s on, 5 s off at high power at 4°C. The average size of sheared DNA was 200 to 500 bp. The cell lysate was collected and centrifuged (20,000 × *g* for 30 min at 4°C) to prepare the cell extract. The amount of total protein was measured by the Bio-Rad protein assay (Bio-Rad) using bovine serum albumin (BSA) as a standard. The cell extract was diluted with FLAG buffer containing protease inhibitor cocktail to reach 0.5 mg/ml total protein. A 150-μl fraction of the cell extract was saved for later analysis (reference DNA). The remainder was subjected to immunoprecipitation with 80 μl of anti-FLAG M2 agarose (Sigma). The mixture was incubated 90 min on a rotating platform at 4°C. The beads were washed five times with FLAG buffer. Immunoprecipitated complexes were eluted from beads by treatment with 240 μl of IP buffer with 100 ng/μl of 3× FLAG-peptide (Sigma). Cross-links of immunoprecipitated samples and of total DNA samples were reversed by incubation overnight at 65°C. Samples were then treated with RNase A and protease K for 2 h at 55°C. DNA was extracted with phenol-chloroform and purified with a QIAquick PCR purification minElute kit (Qiagen). DNA samples were blunted with T4 DNA polymerase, ligated to linkers, and amplified by PCR. Amplified DNAs from reference DNA and immunoprecipitated DNA were differentially labeled with cyanine 3 (Cy3) and Cy5, respectively, by using a CGH labeling kit (Life Technologies) according to the manufacturer's instructions.

We used the Agilent eArray platform (Agilent Technologies, Palo Alto, CA, USA) to design a *C. glutamicum* oligonucleotide microarray. Two sets of probes were designed. One was used for global gene expression analysis, and the other was for ChIP-chip analysis. For global gene expression analysis, a set of 60-mer oligonucleotide probes specific for all the open reading frames (ORFs) on both the chromosome and a plasmid pCGR1 was designed and synthesized in duplicate (for a total of 6,742 probes). For ChIP-chip analysis, a set of 60-mer oligonucleotide probes covering the entire chromosome (on average, one probe for every 170 bases), was designed (yielding 18,462 and 18,449 probes on the plus strand and the minus strand, respectively). The regions for RNA genes, including rRNA and tRNA, were excluded to avoid biased signals because these regions repeatedly contain similar sequences. In addition, the region highly transcribed often causes false positives in the ChIP-chip analysis (33). Each array contains both probe sets.

Hybridization was performed using the Agilent Oligo aCGH hybrid-

TABLE 2 Primers used in this study

Primer	Sequence (5′–3′)	Purpose
JW102	GCGGTGACCCGGGAGATCTGAATTC	ChIP-chip
LlacZ1291F	CGGTAGAATTCGAGCTCGGTACCT	EMSA
Cy3-llacZ-R[a]	ACGTTGTAAAACGACGGGATC	EMSA
gnd-F	CCACCGACGCAGTCATCA	qRT-PCR
gnd-R	TGATGTCGCCTTCGTCCAT	qRT-PCR
16S rRNA-F	TCGATGCAACGCGAAGAAC	qRT-PCR
16S rRNA-R	GAACCGACCACAAGGGAAAAC	qRT-PCR
EcoRV-icd–400F	CGCGATATCGCCTCCATCACTGTGAAGTG	Promoter-lacZ construction
EcoRV-icd-15R	CGCGATATCAATGATCTTGGCCATGAGTCTC	Promoter-lacZ construction
EcoRV-gapB–400F	CGCGATATCGGTGTCCTCTCGCGCA	Promoter-lacZ construction
EcoRV-gapB-15R	CGCGATATCGATCAACGGCACCATGTCCTC	Promoter-lacZ construction
EcoRV-pyk–390F	CGCGATATCGTCTCCGCAGTAGTGTTTG	Promoter-lacZ construction
EcoRV-pyk-15R	CGCGATATCTCTATCCACGCCCATAAGCCT	Promoter-lacZ construction
EcoRV-maeB–410F	CGCGATATCAAGTGGGTATCGCGTCTGG	Promoter-lacZ construction
EcoRV-maeB-15R	CGCGATATCCAGGTCGATGGTCATATCATTTAGC	Promoter-lacZ construction
BglII-icd–246R	CGCAGATCTTCTTTTCTCCCGTGGAAGAGTAC	Promoter-lacZ construction
BglII-icd–240F	CGCAGATCTCAAGTCGAGCTCGCGG	Promoter-lacZ construction
BglII-gapB–289R	CGCAGATCTCATTGGGTTGAGATATGGGTAC	Promoter-lacZ construction
BglII-gapB–275F	CGCAGATCTTTGCGTAAGGCGGCAG	Promoter-lacZ construction
BglII-pyk–40R	CGCAGATCTCATTAATTCTCGATGAATCTTGC	Promoter-lacZ construction
BglII-pyk–34F	CGCAGATCTCCTGTGGCTTGAGGGGGA	Promoter-lacZ construction
EcoRV-maeB-mut GntR1-site2R	CGCGATATCCAGGTCGATGGTCATTAAGCGTAGCCTTGTTAATCGGTG	Promoter-lacZ construction
BglII-maeB–205R	CGCAGATCTCTTTTGGGTGGTTTTGGGGT	Promoter-lacZ construction
BglII-maeB–194F	CGCAGATCTCAAACAATTAAATTCATCACAAAACAC	Promoter-lacZ construction
LlacZLR-4354F	ATAACCGGGCAGGGGTCTAG	Promoter-lacZ construction
Ind7insert-checkR	GCGTCACGAACAACAGACAGC	Promoter-lacZ construction
LlacZLR-6425R	CGACGGCCAGTGCCAAGC	Promoter-lacZ construction
Ind7insert-checkF	CGAGACTGGAATTGAGGCTC	Promoter-lacZ construction
NheI-2434–1500–F5	GCGGCTAGCGTGCACGGATTCCATGAAC	gntR1-FLAG construction
SalI-2434–1500-R4	GCGGTCGACAAAGCCGAGGAAACAAGAGCAGG	gntR1-FLAG construction
C_gntR_FLAG-tag_nheI	CGCGCTAGCTTACTTGTCATCGTCATCCTTGTAGTCTGCTGCTCCGTTCAGCGTGCCCAGC	gntR1-FLAG construction
C_nheI_gnt3′_ver4	GCGGCTAGCCGATATCGCTAAGAGCTTCAACGA	gntR1-FLAG construction

[a] Cy3 labeled at the 5′ end.

ization kit according to the manufacturer's manual (Agilent). Equal amounts (2.5 μg) of each labeled DNA were mixed and hybridized to microarrays in an Agilent Technologies microarray chamber at 65°C for 24 h in a rotating Agilent hybridization oven at 20 rpm. After hybridization, microarrays were washed with Oligo aCGH/ChIP-on-chip wash buffer 1 (Agilent) at room temperature for 5 min, with Oligo aCGH/ChIP-on-chip wash buffer 2 (Agilent Technologies) at 31°C for 5 min, with acetonitrile for 10 s, and with a stabilization and drying solution (Agilent) for 30 s at room temperature. Slides were scanned immediately after washing by placement within an Agilent ozone barrier slide cover with the Agilent DNA microarray scanner (G2505C) at a resolution of 5 μm using the two-color scan setting for the 4x44K (Agilent) array slides. Scanning was done in both channels, and the photomultiplier tube (PMT) was set to 100% for both Cy3 and Cy5 channels. The scanned images were quantified with Feature Extraction Software 10.5.5.1 (Agilent) using default parameters (protocol GE2_105_Dec08). Log_2 ratios for each probe were determined as rProcessedSignal/gProcessedSignal (Cy5/Cy3). The entire procedure was carried out two times. Creation of plots of the log_2 ratios against probe location, extraction of ChIP-chip peaks, and determination of genomic locations for the peaks were performed using MochiView v 1.45 (34). Peak extraction was performed using the following setting: for smoothing, smoothing window flank span, 500 bp; minimum weighted location count for inclusion, 1.01; maximum gap for data interpolation, 100 bp; for peak-finding setting, 1st pass filter; peak location width, 250 bp; minimum value for peak inclusion, 0.5; second-pass filter scan distance, 700 bp; minimum peak height change, 0.6; minimum distance between peak midpoint, 200 bp; number of significance sampling, 0. The chromosomal sequences corresponding to the ChIP-chip peaks were extracted and analyzed using multiple Em for motif elicitation (MEME)-ChIP (35) to define the GntR1 consensus sequence. The ChIP-chip peak regions were manually searched for the conserved sequence motif obtained (AWWGGTMRYACCWWT) to find additional consensus sequences. The enrichment factor for a given gene was defined as the log_2 ratio of each peak. These data analyses were performed using one of two ChIP-chip data sets, and reproducibility was checked in the other data set.

Electrophoretic mobility shift assay. The histidine-tagged GntR1 proteins was expressed in *E. coli* and purified as described previously (14). Briefly, overexpression of the histidine-tagged protein was achieved by using a cold shock-expressing vector pCold I system (TaKaRa). *E. coli* cells harboring the resultant plasmid were grown at 37°C in 100 ml of LB medium with ampicillin (50 ng/ml) to an OD_{610} of 0.5. Cultures were incubated for 30 min at 15°C, and then IPTG (isopropyl-β-D-thiogalactopyranoside) was added at a final concentration of 0.1 mM. After 24 h of culture, cells were harvested by centrifugation and suspended in 900 μl of His binding buffer (0.5 M NaCl, 20 mM Tris-HCl, 5 mM imidazole, pH 7.9) (Novagen), 100 μl of Fast Break cell lysis reagent (Promega), and 0.2 mg of lysozyme. The mixture was incubated for 15 min at room temperature, centrifuged for 5 min at 12,000 × *g*, and the supernatant was pooled. The histidine-tagged protein was purified using the His Bind resin and buffer kit (Novagen) according to the procedure specified by the manufacturer. Purification of histidine-tagged GntR1 was checked by SDS-PAGE and Coomassie brilliant blue (CBB) staining (see Fig. S3 in the

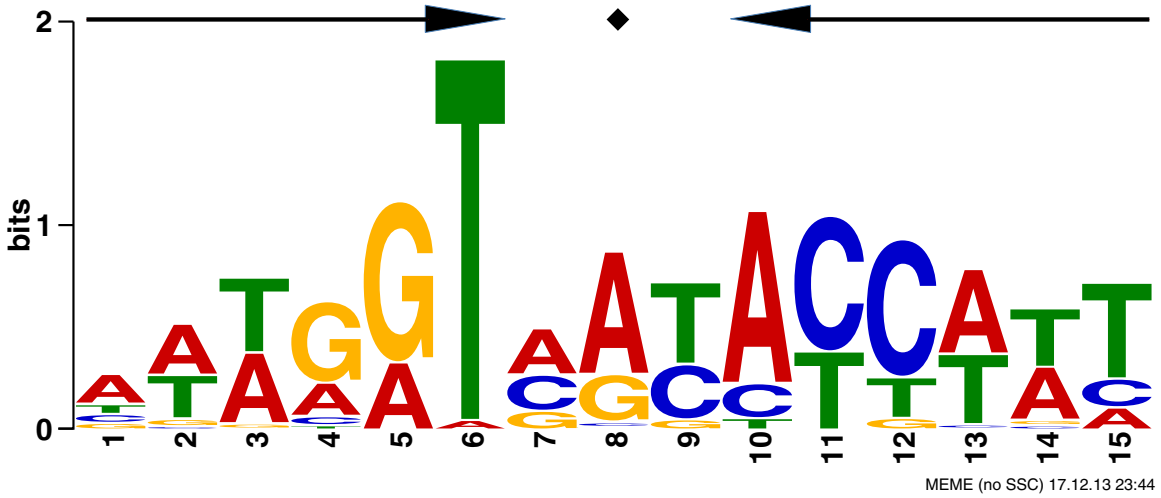

FIG 1 Prediction of GntR1 consensus binding motif. A conserved motif was identified using the MEME algorithm by analyzing the regions with enrichment factors of >2.0 in the ChIP-chip experiment. The size of each letter indicates the relative abundance at the respective position in the consensus matrix generated with MEME. The palindromic sequence is depicted by symmetrical arrows.

supplemental material). A single band corresponding to the size of GntR1 (28 kDa) was observed.

EMSA was carried out in a total volume of 20 μl of binding buffer, consisting of 20 mM Tris-HCl (pH 7.9), 100 mM NaCl, 3 mM $MgCl_2$, 0.1 mM EDTA, 0.1 mM dithiothreitol (DTT), 5% glycerol, and 50 μg/ml poly(dI-dC), and 50 μg/ml bovine serum albumin. The Cy3-labeled promoter DNA fragment was amplified by PCR using primers listed in Table 2 and genomic DNA of the wild-type strain or a strain carrying the mutated GntR1 binding site as the template. The DNA fragment (2 nM) was incubated with the purified GntR1 protein for 10 min at 25°C. The mixture was fractionated by electrophoresis on a native 5% polyacrylamide gel containing 5% glycerol in 0.5× Tris-borate EDTA (TBE; 45 mM Tris-borate, pH 8.0, 1 mM EDTA) at room temperature.

DNA microarray analysis. *C. glutamicum* R wild-type cells and cells with *gntR1* deleted were grown aerobically in nutrient-rich A medium supplemented with 2% (wt/vol) glucose. Total RNA was isolated from exponentially growing cells (OD_{610}, 2.0) using the Nucleo Spin RNA (Macherey-Nagel). For transcriptome analysis, the cDNAs were reverse transcribed from 10 μg of total RNAs and labeled with cyanine 3 (Cy3) using the SuperScript Indirect cDNA labeling system (Life Technologies). Hybridization was performed using the gene expression hybridization kit according to the manufacturer's manual (Agilent). The labeled cDNA was hybridized to microarrays in an Agilent Technologies microarray chamber at 65°C for 17 h in a rotating Agilent hybridization oven. After hybridization, microarrays were washed with GE wash buffer 1 (Agilent) at room temperature for 1 min and with GE wash buffer 2 (Agilent) at 37°C for 1 min. Slides were scanned immediately after washing on the Agilent DNA microarray scanner (G2505C) at a resolution of 5 μm, using the single-color scan setting for 4x44k array slides. PMT was set to 100% for Cy3 channels. The scanned images were quantified with Feature Extraction Software 10.5.5.1 (Agilent) using default parameters (protocol GE1_105_Dec08). Feature extracted data were analyzed using GeneSpring GX v 12.0 software from Agilent. Normalization of the data was done in GeneSpring GX using the recommended percentile shift normalization (50th percentile). The resultant data were expressed as averages of mRNA ratios (Δ*gntR1* mRNA/WT mRNA) from three independent experiments. Genes that showed significantly altered mRNA levels (*P* value of <0.02 in a Student *t* test), by a factor of 1.5 or more, were identified and are listed in Table S2 in the supplemental material.

β-Galactosidase assay. For the β-galactosidase assay, *C. glutamicum* R was grown to an OD_{610} of 2.0, and 1 ml of culture samples was harvested and dissolved in 1 ml of Z buffer (Na_2H or NaH_2PO_4 [pH 7.0], 10 mM KCl, 1 mM $MgSO_4$, 50 mM β-mercaptoethanol) with 2% toluene to permeabilize the cell. β-Galactosidase activity was determined with permeabilized cells as described previously (17).

Microarray data accession number. The microarray and ChIP-chip data have been submitted to the NCBI Gene Expression Omnibus (GEO) functional genomics data repository under the accession number GSE58633.

RESULTS

Identification of *in vivo* binding sites of GntR1. A genome-wide search for the binding region of GntR1 was conducted by ChIP-chip analysis using a strain in which the chromosomally encoded *gntR1* was modified to add the FLAG tag at its C terminus (strain TI01). TI01 and the wild-type strain showed the same *gnd* mRNA expression level, in contrast to the upregulation of this gene by *gntR1* deletion, indicating that the FLAG-tagged GntR1 is functional *in vivo* (see Fig. S1 in the supplemental material). To determine the target region of GntR1, TI01 was grown in the nutrient-rich A medium supplemented with 2% (wt/vol) glucose, and the DNA fragments binding to GntR1 were collected. GntR1 is expected to be in the active form under the experimental conditions, because the expression of *gnd* mRNA is in a repressed state and deletion of *gntR1* relieved this repression under the growth conditions (14). ChIP and microarray analysis was performed as described in Materials and Methods, and regions that were considered possible GntR1 target regions are listed in Table S1 in the supplemental material. Under the stricter conditions whereby the regions exhibiting enrichment factors of >2.0 were selected, we identified 56 regions that are very likely to be the *in vivo* GntR1 binding sites, and these regions were selected for further analysis. Of these regions, 51 sites are located upstream of coding sequences, suggesting that GntR1 regulates transcription of these genes. The identified 56 sites include the upstream regions of genes *gntP*, *gntK*, *gnd*, *tkt*, *ptsG*, *ptsS*, and *pckA*, the regions that GntR1 was shown to bind to *in vitro* (13–15).

A MEME (multiple Em for motif elicitation) (19) alignment of the putative GntR1 binding regions produced the conserved sequence 5′-AWWGGTMRYACCWWT-3′ (Fig. 1), which is found in all the regions identified in the ChIP-chip analysis. The se-

TABLE 3 Carbon metabolic genes identified in ChIP-chip analysis[a]

Gene ID	Gene name	Enrichment factor[b]	DNA microarray ratio[c]	GntR1 binding motif (5′–3′)	Function
cgR_1513	*gnd*	5.66	3.65	AAAGGTGTGACCATT	6-Phosphogluconate dehydrogenase
cgR_2397	*gntV*	5.19	60.60	ATTGGTACTATCATA	Gluconate kinase
cgR_1973	*pyk*	5.14	1.34	ACAGGTACTACCATT	Pyruvate kinase
cgR_0261	*iolT1*	5.06	0.74	ATTGGTAATACTTAG	Metabolite transport protein
cgR_0402	*bglS*	5.01	10.72	AAAGGGATTACCATT	Putative beta-glucosidase
cgR_2751	*pckA*	4.91	0.42	AAAGGGATTACCATT	Phosphoenolpyruvate carboxykinase
cgR_2895	*maeB*	4.67	0.48	AATGATATGACCATC	Malic enzyme
cgR_2262	*mdh*	4.64	0.85	GATGGTGTTACCTTT	Malate dehydrogenase
cgR_1425	*ptsG*	4.54	0.29	AAAAGTATTACCTTT	Phosphotransferase, glucose-specific enzyme II
cgR_1624	*tkt*	4.46	1.82	AAAGGTGTGACCAAT	Transketolase
cgR_2806	*gntP*	4.32	2.79	ATTAGTATGATCAAA	Gluconate permease
cgR_2497	*dctA*	4.25	4.17	ATTAATATTACCTTT	Na^+/H^+-dicarboxylate symporter
cgR_1636	*gapA*	4.24	1.23	ATTGGGATTACCATT	Glyceraldehyde-3-phosphate dehydrogenase
cgR_2454		4.20	9.01	TTAGGTGTGATCTTT	Sugar phosphate isomerase/epimerase
cgR_1038	*gapB*	4.14	0.31	AAAGATGTGATCATT	Glyceraldehyde 3-phosphate dehydrogenase
cgR_2451		3.91	2.40	ATTAGTGTGACCAAA	Na^+/H^+-dicarboxylate symporter
cgR_2222	*dctP1*	3.49	7.77	AAAGGGATCACCATT	Putative C4-dicarboxylate-binding protein
cgR_2896	*gntK*	3.18	1.83	AAAGGTCTGACTAAT	Putative gluconate kinase
cgR_2120	*aceE*	3.09	0.95	TTAGGTACGACCAAA	Pyruvate dehydrogenase
cgR_0784	*icd*	2.52	1.07	CTTGGTGTGATCTTT	Isocitrate dehydrogenase
cgR_2547	*ptsS*	2.29	1.69	AATAGTGCCACCTTT	Enzyme II sucrose protein

[a] All ChIP-chip peaks were located upstream of the genes listed in the Gene ID column.
[b] Relative peak height ratios of the array data in the ChIP DNA to input DNA are shown in the base 2 logarithm.
[c] Relative ratios of the transcript levels in the *gntR1*-deleted cells to those in the wild-type strain were determined by DNA microarray analysis.

quence is a 6-3-6-bp inverted repeat with high conservation of T at the 6th position. The sequence is found in the GntR1 binding region within the *gntK* and *gnd* promoters that has been experimentally tested by DNase I footprinting assay (13, 14), strongly indicating that the motif is the recognition sequence for GntR1 binding.

Transcriptome analysis of the effects of *gntR1* gene deletion. The results of ChIP-chip analysis indicate that GntR1 may be involved in the regulation of many more genes than previously assumed. Therefore, we conducted transcriptome analysis using a DNA microarray. *C. glutamicum* WT and a *gntR1* deletion strain were grown in nutrient-rich A medium supplemented with 2% (wt/vol) glucose. Total RNA was extracted from the logarithmic grown cells and subjected to microarray analysis, and the mRNA expression levels in the *gntR1* deletion strain were compared to those in the wild-type strain. Seventy genes were upregulated more than 1.5-fold, whereas 229 genes were downregulated more than 1.5-fold (see Table S2 in the supplemental material). Decreased expression of *ptsG* and *pckA* and increased expression of *tkt*, *gnd*, *gntK*, *gntP*, and *gntV* were observed as described previously (13–15). In addition to these genes, we found that the expression of many of the genes involved in carbon metabolism was changed; these genes are *gapB*, *rbsK2*, *rbsK1*, *dctP2*, *ugpE*, *dhaS*, *maeB*, *dctA*, *dctM1*, *dctP1*, *bglF2*, and *bglF*. In Table 3, carbon metabolism genes identified in ChIP-chip analysis are presented with transcriptome data. The genes that were highly enriched by ChIP tend to show a large change in the expression by deletion of *gntR1*, although expression of some of the ChIP-enriched genes was not significantly changed. Therefore, we further investigated the role of GntR1 on the expression of carbon metabolism genes that showed high enrichment by ChIP-chip with altered or unaltered mRNA levels in transcriptome data as follows.

Binding of GntR1 to the promoter regions of *icd*, *gapB*, *pckA*, and *maeB* genes. To explore the more detailed view of the GntR1-mediated regulation, we selected the carbon metabolism genes that were newly identified in the ChIP-chip analysis, and the GntR1 binding motif was found within the 500 bp from the translation initiation codon (*icd*, *gapB*, *pyk*, and *maeB*). The microarray results showed that *gntR1* deletion resulted in the reduction in the *gapB* and *maeB* transcripts, whereas transcriptional levels of *icd* and *pyk* were not significantly changed by *gntR1* deletion. To test the binding of GntR1 to the promoter region of these genes, we conducted EMSA with purified GntR1 protein. We prepared the DNA fragment with or without mutation (see Fig. S2 in the supplemental material) at the putative GntR1 binding motif as a probe used for EMSA (Fig. 2A). Incubation of these probes corresponding to the wild-type upstream regions of *icd*, *gapB*, and *pyk* with GntR1 protein resulted in a DNA-protein complex. EMSA using their mutated DNA probes showed no complex with GntR1. These results indicate that GntR1 specifically binds to the predicted site and also verify the accurate prediction of the GntR1 binding motif (Fig. 1). Upstream of the *maeB* gene, there are two possible GntR1 binding sites, one located upstream of the transcription start site and the other overlapping the translational start codon. Indeed, addition of GntR1 resulted in the two shifted bands detected in EMSA. Mutation either in the mut1 site or in the mut2 site (see Fig. S2 in the supplemental material) resulted in one shifted band, and the mutation at both sites resulted in the complete disappearance of shifted bands. These results indicate that there are two GntR1 binding sites within the *maeB* promoter region. Binding affinity of GntR1 to *gntK* promoter region is diminished in the presence of gluconate or glucono-δ-lactone (13). We then tested whether gluconate affects the binding of GntR1 to the *gapB*, *pyk*, *icd*, and *maeB* promoters (Fig. 2B). As expected, the

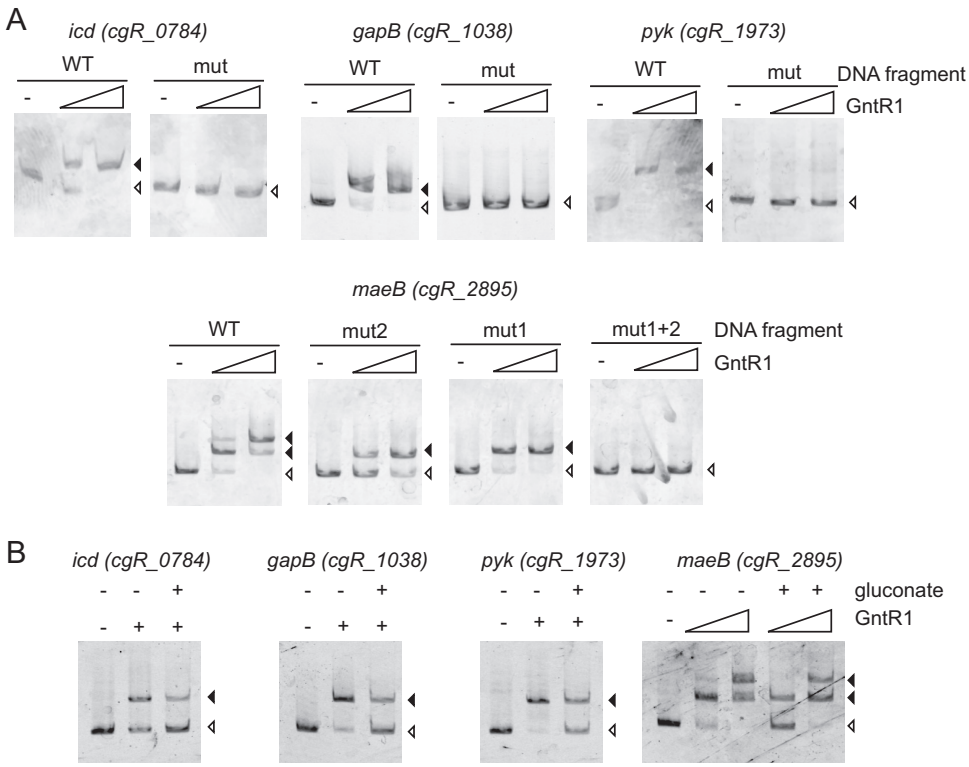

FIG 2 Binding of GntR1 to the promoter regions of the predicted target genes. (A) The DNA fragment (2 nM) with or without mutation at putative GntR1 binding sites was incubated with 0, 15, and 60 nM GntR1. DNA fragments complexed with GntR1 are indicated by closed arrowheads, and free DNA is indicated by an open arrowhead. (B) Effects of gluconate on the binding of GntR1 to target promoters. The promoter DNA fragments of *icd*, *gapB*, and *pyk* were incubated with 15 nM GntR1. The DNA fragment of *maeB* was incubated with 0, 15, and 60 nM GntR1. DNA binding reactions were performed in the presence or absence of 50 mM gluconate.

GntR1 band shift was diminished in the presence of 50 mM gluconate. However, gluconate did not completely inhibit the GntR1 binding to these promoter DNAs, as observed in the *gntK* promoter.

Effects of mutation at GntR1 binding site on the promoter activity of *icd*, *gapB*, *pyk*, and *maeB*. To investigate the role of GntR1 on the promoter activity of *icd*, *gapB*, *pyk*, and *maeB*, we constructed the translational promoter-*lacZ* fusions with or without mutation at the GntR1 binding site and integrated them into the chromosome of *C. glutamicum* R. The strains were grown in nutrient-rich A medium with 2% glucose or 2% gluconate or 1% glucose plus 1% gluconate, and the promoter activity of the exponentially growing cells was determined by analyzing the β-galactosidase activity (Fig. 3). The activity of the *icd* promoter carrying the mutation at the GntR1 binding site was less than one-half that of the wild-type promoter both in the presence and in the absence of gluconate. The promoter activity of *gapB* was also decreased by a mutation of the GntR1 binding site in cells grown in the absence of gluconate. In the gluconate-grown cells, there was no difference between the wild type and the GntR1 binding site mutant. In contrast to *icd* and *gapB*, the *pyk* promoter activity was increased about 3.5-fold by the GntR1 site mutation. A slight increase in wild-type *pyk* promoter activity was observed in the presence of glucose and gluconate. Mutation at each or both of the two GntR1 sites in the *maeB* promoter resulted in the marked decrease in the promoter activity both in the presence and in the absence of gluconate. These results suggest that GntR1 activates the promoters of *icd*, *gapB*, and *maeB*, whereas GntR1 represses the *pyk* promoter. Expression of *gapB* and *maeB* were decreased by deletion of *gntR1* (Table 3), which supports the idea that GntR1 is an activator of *gapB* and *maeB*. Gluconate reduced the GntR1-mediated activation of the *gapB* promoter. The effect of gluconate on the *pyk* promoter was modest and was not observed in *icd* and *maeB*. These results suggest that gluconate partially inhibited GntR1 activity, which affects target promoter activities to various extents.

DISCUSSION

GntR1/2 is known to control the expression of genes of gluconate utilization (*gntP* and *gntK*), the pentose phosphate pathway (*tkt*, *tal*, *zwf*, *opcA*, *devB*, and *gnd*), the phosphotransferase system (*ptsG* and *ptsS*), and gluconeogenesis (*pckA*) in *C. glutamicum* ATCC 13032, indicating that GntR1/2 is one of the important transcriptional regulators for carbon metabolism (13–15). In *C. glutamicum* R, the *gntR2* gene is missing and *gntR1* is solely responsible for the induction of the *gnd* gene by gluconate (14). In this study, we conducted ChIP-chip analysis to explore the genome-wide binding target of GntR1 *in vivo*. In the ChIP-chip analysis, 56 regions, including all the seven previously identified GntR1 binding sites, were enriched by GntR1, indicating that many more genes are under the control of GntR1 than previously thought. The marked increase of the GntR1 target site by ChIP-chip analysis allowed us to predict a more precise consensus sequence of the GntR1 binding sites (Fig. 1). The predicted sequence forms an inverted repeat, which is not obvious in the previous

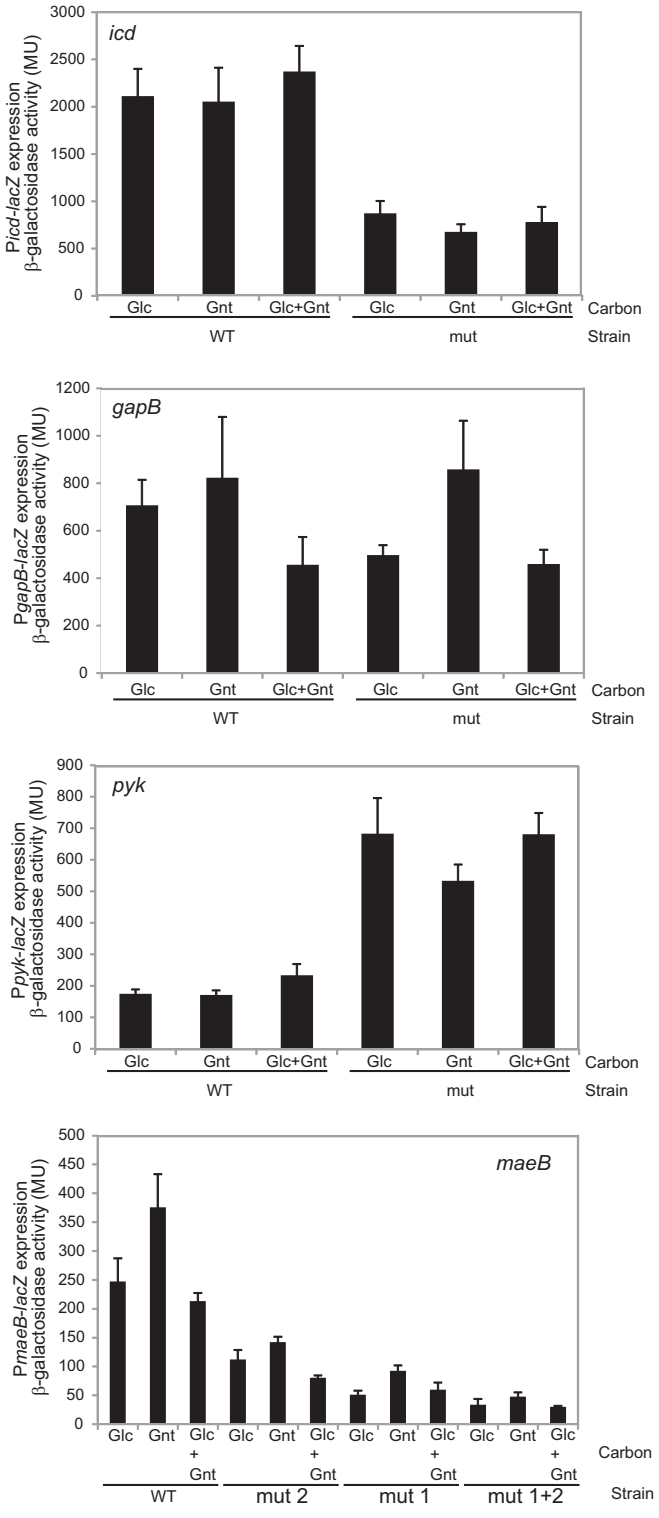

FIG 3 Effects of the mutation at GntR1 binding sites on the promoter activity of the predicted target genes. The strains containing *icd*, *gapB*, *pyk*, or *maeB* promoter-*lacZ* fusion with or without mutations at GntR1 binding sites were grown in nutrient-rich A medium supplemented with 2.0% (wt/vol) glucose or 2.0% gluconate or 1.0% glucose plus 1.0% gluconate. Culture samples were taken at an OD_{610} of 2.0, and β-galactosidase activities were determined. The values are the means of results from three independent experiments, and standard deviations are indicated.

report (13). Mutation at the consensus sequence effectively eliminated the binding of GntR1 (Fig. 2), supporting the accurate prediction of the binding motif.

Transcriptome analysis of the effect of *gntR1* deletion showed that expression of 70 genes was increased, whereas expression of 193 genes was decreased (see Table S2 in the supplemental material). As expected, expression of the genes encoding gluconate utilization and the pentose phosphate pathway was increased, and expression of *ptsG* and *pckA* was decreased by the deletion of *gntR1*. However, expression of the *ptsS* gene, which showed decreased expression in the *gntR1*- and *gntR2*-deleted strain in a previous paper (13), showed increased expression in our microarray analysis. This inconsistency may be caused by the different growth media used in the studies and requires more-extensive analysis to determine the role of GntR1 on the regulation of *ptsS*. Among the genes listed in Table S2 in the supplemental material, 23 genes, including *ptsG*, *pckA*, *ptsS*, *tkt*, *gntP*, *gnd*, and *gntV*, were also detected as probable direct targets of GntR1 in ChIP-chip analysis. Of the 23 genes, the GntR1 binding peak was located within the intergenic region of four sets of divergently oriented genes, i.e., *cgR_1513* (*gnd*)-*cgR1514*, *cgR_1623* (*ctaB*)-*cgR_1624* (*tkt*), *cgR_6135-cgR_2388* (*betT*), and *cgR_2646-cgR_2647*, suggesting that binding of GntR1 to the intergenic region simultaneously controls its downstream genes. Many genes showed different expression by *gntR1* deletion in microarray, but their upstream regions showed no significant interaction with GntR1 in ChIP-chip analysis. Thus, it is likely that these genes are indirectly controlled by GntR1. In this context, it is noteworthy that, as shown by ChIP-chip analysis, GntR1 binds upstream of *cgR_0453* and *cgR_2263*, both encoding TetR family transcriptional regulators. Upregulation of *cgR_2263* mRNA by *gntR1* deletion was also observed in microarray analysis. Although the regulatory target of these transcriptional regulators has not been reported, GntR1 may indirectly affect the expression of a number of genes by controlling the expression of these regulators. Another possible indirect effect by *gntR1* deletion may be due to the reduced glucose utilization. The glucose uptake rate of a *gntR1* and *gntR2* double deletion strain was about one-third that of the wild-type strain (13), which is probably the result of reduced expression of the *ptsG* gene. Decreased glucose utilization may relieve the catabolite repression by glucose. For example, *bglF-bglA-bglG* genes, coding for the β-glucoside catabolic genes, are under strict control of glucose repression (20). Therefore, increased expression of the *bglF-bglA-bglG* genes may be the result of weakened glucose repression.

We selected four carbon metabolism genes (*icd*, *gapB*, *pyk*, and *maeB*) for further analysis of the regulation by GntR1. These genes are known to be controlled by several transcriptional regulators. For example, expression of *gapB* and *maeB* are diminished in a *ramA*-deleted strain while *pyk* expression is increased. Binding of RamA to the promoter region of *gapB*, *maeB*, and *pyk* was confirmed by EMSA (21, 22). Expression of *pyk* was also increased in a *sugR* mutant, and binding of SugR to the *pyk* promoter region was confirmed by EMSA (23). Expression of *maeB* is subject to complex regulation. Promoter activity is downregulated by RamB, the TetR-type regulator MalR, and AmtR, a master regulator of nitrogen regulation (22). However, participation of GntR1 in the regulation of these genes has not been reported. Binding of GntR1 to the promoter region of these genes was observed by EMSA, confirming the ChIP-chip result (Fig. 2). Mutations at the predicted GntR1 binding consensus sequence resulted

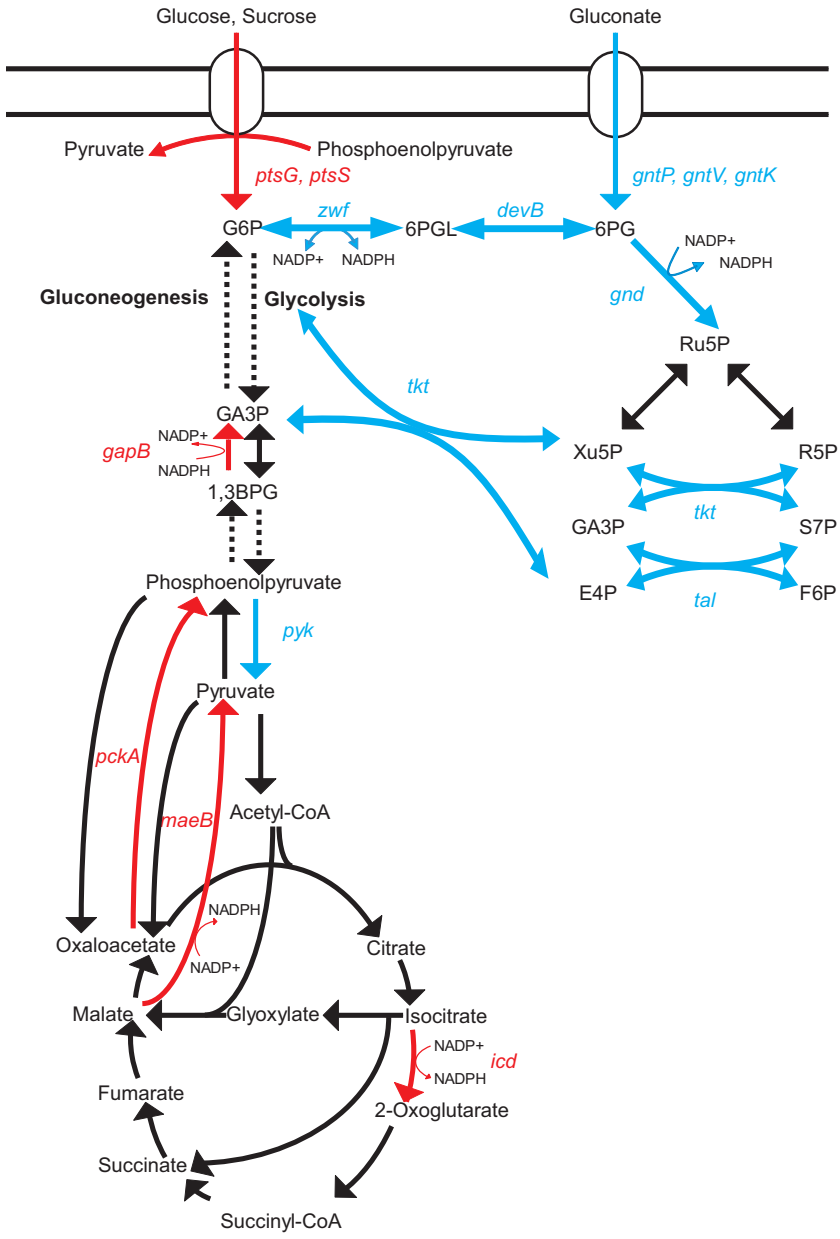

FIG 4 Model of the regulation of carbon catabolic genes by GntR1 in *C. glutamicum*. Metabolic pathways and genes activated by GntR1 are in red, while blue indicates repression. Abbreviations: G6P, glucose 6-phosphate; 6PGL, 6-phospho glucono 1,5-lactone; 6PG, 6-phospho gluconate; Ru5P, ribulose 5-phosphate; Xu5P, xylulose 5-phosphate; R5P, ribose 5-phosphate; GA3P, glyceraldehyde 3-phosphate; S7P, sedoheptulose 7-phosphate; F6P, fructose 6-phosphate; E4P, erythrose 4-phosphate.

in the disappearance of the shifted bands, indicating that the binding is specific and the predicted GntR1 consensus sequence is reliable.

Promoter-reporter analysis of the *icd*, *gapB*, *pyk*, and *maeB* genes with or without mutation at the GntR1 binding site indicates that GntR1 is an activator of *icd* and *gapB* while GntR1 is a repressor of *pyk*. In the *maeB* promoter, mutation at both of the GntR1 binding sites resulted in reduced promoter activity, consistent with the microarray data, which showed deletion of the *gntR1* gene reduced the mRNA level of *maeB* to about one-half of the level in the wild-type strain. The transcription start sites of *icd*, *gapB*, and *maeB* were determined previously (see Fig. S2 in the supplemental material) (24, 25). The GntR1 binding sites of *icd*, *gapB*, and *maeB* site 1 are located upstream of the transcription start site, which is in accord with the activation of these promoters by GntR1. However, *maeB* site 2 overlaps the translation start codon (see Fig. S2 in the supplemental material); therefore, caution is needed in interpreting the result of *maeB* site 2 mutation. Although the translation initiation codon was avoided for mutation, it may affect the recognition of ribosomes to *maeB-lacZ* mRNA, leading to the defect in translation. Experiments such as *in vitro* transcription analysis of GntR1 with the site 2-mutated *maeB* promoter may reveal whether binding of GntR1 to site 2 causes activation of the *maeB* promoter.

DNA binding affinity of GntR1 to the *gntK* promoter is decreased by gluconate and glucono-δ-lactone (13). Similarly, the binding of GntR1 to *icd*, *gapB*, *pyk*, and *maeB* promoter DNA is partially inhibited by gluconate (Fig. 2B). Gluconate eliminated the effect of GntR1 activation for the *gapB* promoter, partially derepressed the *pyk* promoter, and showed no obvious effect on *icd* and *maeB* promoters (Fig. 3). The different effects of gluconate on these promoters *in vivo* may be caused by the interactions of other transcriptional regulators as mentioned above. The regulation of carbon metabolism genes by GntR1 is summarized in Fig. 4. The DNA binding activity of GntR1 is diminished by gluconate or glucono-lactone, indicating that GntR1 acts as a sensor of the presence or absence of these sugar molecules (13). In agreement with this, a DNA fragment of gluconate catabolic genes was highly enriched by ChIP-chip analysis, and these genes showed a strong increase in mRNA level in the *gntR1*-deleted strain (see Table S2 in the supplemental material). In the absence of gluconate, GntR1 represses the gluconate utilization system and the pentose phosphate pathway but activates the glucose and sucrose uptake (13). These regulations are thought to balance the utilization of gluconate with glucose or sucrose in *C. glutamicum*. What is the role of GntR1 in the regulation of other carbon metabolism genes? *pyk* is downregulated, while *pckA* is upregulated by GntR1 (Fig. 4). These regulations, together with the activation of *ptsG* and *ptsS*, should support PEP-dependent uptake of glucose and sucrose in the absence of gluconate. Indeed, the consumption of glucose is lowered by *gntR1* and *gntR2* deletion (13). In addition to the regulation of *pyk* and *pckA*, upregulation of *gapB* and *maeB* by GntR1 may improve fitness in the presence of carbon sources other than gluconate and PTS-sugar by facilitating gluconeogenesis. It is also noteworthy that *icd* and *maeB* positively compensate for the function of the pentose phosphate pathway in the generation of NADPH in *C. glutamicum* (26–28). Thus, it is conceivable that the GntR1 plays a role in coordinated utilization of gluconate and other carbon sources. Further studies on the involvement of GntR1 in gluconeogenesis will be of interest, because in this pathway the *gapB* gene product consumes NADPH rather than generating it. The carbon metabolic flux of *C. glutamicum* has been intensely studied; for example, supply of NADPH, change in the flux of pyruvate node, and on-and-off gluconeogenesis (29–31). Our results imply a GntR1-dependent fine-tuning of these fluxes at the transcriptional level. Advances in understanding of the unique transcriptional regulatory network consisting of various carbon metabolism genes under the control of GntR1/2 along with SugR, RamA, RamB, GlxR, etc., should be valuable for fine-tuning of bioprocesses using this industrially important microorganism.

ACKNOWLEDGMENTS

We thank C. A. Omumasaba (RITE) for critical reading of the manuscript. We thank K. Toyoda for valuable advice on microarray data analysis.

This work was partially supported by a grant from the New Energy and Industrial Technology Development Organization (NEDO).

REFERENCES

1. **Kalinowski J, Bathe B, Bartels D, Bischoff N, Bott M, Burkovski A, Dusch N, Eggeling L, Eikmanns BJ, Gaigalat L, Goesmann A, Hartmann M, Huthmacher K, Krämer R, Linke B, McHardy AC, Meyer F, Möckel B, Pfefferle W, Pühler A, Rey DA, Rückert C, Rupp O, Sahm H, Wendisch VF, Wiegräbe I, Tauch A.** 2003. The complete Corynebacterium glutamicum ATCC 13032 genome sequence and its impact on the production of L-aspartate-derived amino acids and vitamins. J. Biotechnol. **104:**5–25. http://dx.doi.org/10.1016/S0168-1656(03)00154-8.
2. **Liebl W.** 2005. *Corynebacterium* taxonomy, p 9–34. *In* Eggeling L, Bott M. (ed), Handbook of *Corynebacterium glutamicum*. CRC Press, Boca Raton, FL.
3. **Inui M, Murakami S, Okino S, Kawaguchi H, Vertès AA, Yukawa H.** 2004. Metabolic analysis of *Corynebacterium glutamicum* during lactate and succinate productions under oxygen deprivation conditions. J. Mol. Microbiol. Biotechnol. **7:**182–196. http://dx.doi.org/10.1159/000079827.
4. **Okino S, Noburyu R, Suda M, Jojima T, Inui M, Yukawa H.** 2008. An efficient succinic acid production process in a metabolically engineered *Corynebacterium glutamicum* strain. Appl. Microbiol. Biotechnol. **81:**459–464.
5. **Okino S, Suda M, Fujikura K, Inui M, Yukawa H.** 2008. Production of D-lactic acid by *Corynebacterium glutamicum* under oxygen deprivation. Appl. Microbiol. Biotechnol. **78:**449–454. http://dx.doi.org/10.1007/s00253-007-1336-7.
6. **Ikeda M, Nakagawa S.** 2003. The *Corynebacterium glutamicum genome*: features and impacts on biotechnological processes. Appl. Microbiol. Biotechnol. **62:**99–109. http://dx.doi.org/10.1007/s00253-003-1328-1.
7. **Yukawa H, Omumasaba CA, Nonaka H, Kós P, Okai N, Suzuki N, Suda M, Tsuge Y, Watanabe J, Ikeda Y, Vertès AA, Inui M.** 2007. Comparative analysis of the *Corynebacterium glutamicum* group and complete genome sequence of strain R. Microbiology **153:**1042–1058. http://dx.doi.org/10.1099/mic.0.2006/003657-0.
8. **Schröder J, Tauch A.** 2010. Transcriptional regulation of gene expression in *Corynebacterium glutamicum*: the role of global, master and local regulators in the modular and hierarchical gene regulatory network. FEMS Microbiol. Rev. **34:**685–737. http://dx.doi.org/10.1111/j.1574-6976.2010.00228.x.
9. **Teramoto H, Inui M, Yukawa H.** 2011. Transcriptional regulators of multiple genes involved in carbon metabolism in *Corynebacterium glutamicum*. J. Biotechnol. **154:**114–125. http://dx.doi.org/10.1016/j.jbiotec.2011.01.016.
10. **Teramoto H, Inui M, Yukawa H.** 2009. Regulation of expression of genes involved in quinate and shikimate utilization in *Corynebacterium glutamicum*. Appl. Environ. Microbiol. **75:**3461–3468. http://dx.doi.org/10.1128/AEM.00163-09.
11. **Wendisch VF, de Graaf AA, Sahm H, Eikmanns BJ.** 2000. Quantitative determination of metabolic fluxes during coutilization of two carbon sources: comparative analyses with *Corynebacterium glutamicum* during growth on acetate and/or glucose. J. Bacteriol. **182:**3088–3096. http://dx.doi.org/10.1128/JB.182.11.3088-3096.2000.
12. **Toyoda K, Teramoto H, Inui M, Yukawa H.** 2011. Genome-wide identification of in vivo binding sites of GlxR, a cyclic AMP receptor protein-type regulator in *Corynebacterium glutamicum*. J. Bacteriol. **193:**4123–4133. http://dx.doi.org/10.1128/JB.00384-11.
13. **Frunzke J, Engels V, Hasenbein S, Gatgens C, Bott M.** 2008. Co-ordinated regulation of gluconate catabolism and glucose uptake in *Corynebacterium glutamicum* by two functionally equivalent transcriptional regulators, GntR1 and GntR2. Mol. Microbiol. **67:**305–322. http://dx.doi.org/10.1111/j.1365-2958.2007.06020.x.
14. **Tanaka Y, Ehira S, Teramoto H, Inui M, Yukawa H.** 2012. Coordinated regulation of *gnd*, which encodes 6-phosphogluconate dehydrogenase, by the two transcriptional regulators GntR1 and RamA in *Corynebacterium glutamicum*. J. Bacteriol. **194:**6527–6536. http://dx.doi.org/10.1128/JB.01635-12.
15. **Klaffl S, Brocker M, Kalinowski J, Eikmanns BJ, Bott M.** 2013. Complex regulation of the phosphoenolpyruvate carboxykinase gene *pck* and characterization of its GntR-type regulator IolR as a repressor of *myo*-inositol utilization genes in *Corynebacterium glutamicum*. J. Bacteriol. **195:**4283–4296. http://dx.doi.org/10.1128/JB.00265-13.
16. **Inui M, Suda M, Okino S, Nonaka H, Puskás LG, Vertès AA, Yukawa H.** 2007. Transcriptional profiling of *Corynebacterium glutamicum* metabolism during organic acid production under oxygen deprivation conditions. Microbiology **153:**2491–2504. http://dx.doi.org/10.1099/mic.0.2006/005587-0.
17. **Tanaka Y, Okai N, Teramoto H, Inui M, Yukawa H.** 2008. Regulation of the expression of phosphoenolpyruvate: carbohydrate phosphotransferase system (PTS) genes in *Corynebacterium glutamicum* R. Microbiology **154:**264–274. http://dx.doi.org/10.1099/mic.0.2007/008862-0.
18. **Inui M, Kawaguchi H, Murakami S, Vertès AA, Yukawa H.** 2004. Metabolic engineering of *Corynebacterium glutamicum* for fuel ethanol

production under oxygen-deprivation conditions. J. Mol. Microbiol. Biotechnol. **8:**243–254. http://dx.doi.org/10.1159/000086705.
19. **Bailey TL, Elkan C.** 1994. Fitting a mixture model by expectation maximization to discover motifs in biopolymers. Proc. Int. Conf. Intell. Syst. Mol. Biol. **2:**28–36.
20. **Tanaka Y, Teramoto H, Inui M, Yukawa H.** 2011. Translation efficiency of antiterminator proteins is a determinant for the difference in glucose repression of two beta-glucoside phosphotransferase system gene clusters in Corynebacterium glutamicum R. J. Bacteriol. **193:**349–357. http://dx.doi.org/10.1128/JB.01123-10.
21. **Auchter M, Cramer A, Hüser A, Rückert C, Emer D, Schwarz P, Arndt A, Lange C, Kalinowski J, Wendisch VF, Eikmanns BJ.** 2011. RamA and RamB are global transcriptional regulators in *Corynebacterium glutamicum* and control genes for enzymes of the central metabolism. J. Biotechnol. **154:**126–139. http://dx.doi.org/10.1016/j.jbiotec.2010.07.001.
22. **Krause JP, Polen T, Youn JW, Emer D, Eikmanns BJ, Wendisch VF.** 2012. Regulation of the malic enzyme gene *malE* by the transcriptional regulator MalR in *Corynebacterium glutamicum*. J. Biotechnol. **159:**204–215. http://dx.doi.org/10.1016/j.jbiotec.2012.01.003.
23. **Engels V, Lindner SN, Wendisch VF.** 2008. The global repressor SugR controls expression of genes of glycolysis and of the L-lactate dehydrogenase LdhA in *Corynebacterium glutamicum*. J. Bacteriol. **190:**8033–8044. http://dx.doi.org/10.1128/JB.00705-08.
24. **Han SO, Inui M, Yukawa H.** 2008. Transcription of *Corynebacterium glutamicum* genes involved in tricarboxylic acid cycle and glyoxylate cycle. J. Mol. Microbiol. Biotechnol. **15:**264–276. http://dx.doi.org/10.1159/000117614.
25. **Han SO, Inui M, Yukawa H.** 2007. Expression of *Corynebacterium glutamicum* glycolytic genes varies with carbon source and growth phase. Microbiology **153:**2190–2202. http://dx.doi.org/10.1099/mic.0.2006/004366-0.
26. **Gourdon P, Baucher MF, Lindley ND, Guyonvarch A.** 2000. Cloning of the malic enzyme gene from *Corynebacterium glutamicum* and role of the enzyme in lactate metabolism. Appl. Environ. Microbiol. **66:**2981–2987. http://dx.doi.org/10.1128/AEM.66.7.2981-2987.2000.
27. **Omumasaba CA, Okai N, Inui M, Yukawa H.** 2004. *Corynebacterium glutamicum* glyceraldehyde-3-phosphate dehydrogenase isoforms with opposite, ATP-dependent regulation. J. Mol. Microbiol. Biotechnol. **8:**91–103. http://dx.doi.org/10.1159/000084564.
28. **Eikmanns BJ, Rittmann D, Sahm H.** 1995. Cloning, sequence analysis, expression, and inactivation of the *Corynebacterium glutamicum icd* gene encoding isocitrate dehydrogenase and biochemical characterization of the enzyme. J. Bacteriol. **177:**774–782.
29. **Kiefer P, Heinzle E, Zelder O, Wittmann C.** 2004. Comparative metabolic flux analysis of lysine-producing *Corynebacterium glutamicum* cultured on glucose or fructose. Appl. Environ. Microbiol. **70:**229–239. http://dx.doi.org/10.1128/AEM.70.1.229-239.2004.
30. **Hoon Yang T, Wittmann C, Heinzle E.** 2006. Respirometric 13C flux analysis. Part II. In vivo flux estimation of lysine-producing *Corynebacterium glutamicum*. Metab. Eng. **8:**432–446. http://dx.doi.org/10.1016/j.ymben.2006.03.002.
31. **Sahm H, Eggeling L, de Graaf AA.** 2000. Pathway analysis and metabolic engineering in *Corynebacterium glutamicum*. Biol. Chem. **381:**899–910.
32. **Toyoda K, Teramoto H, Inui M, Yukawa H.** 2009. Involvement of the LuxR-type transcriptional regulator RamA in regulation of expression of the *gapA* gene, encoding glyceraldehyde-3-phosphate dehydrogenase of *Corynebacterium glutamicum*. J. Bacteriol. **191:**968–977. http://dx.doi.org/10.1128/JB.01425-08.
33. **Waldminghaus T, Skarstad K.** 2010. ChIP on Chip: surprising results are often artifacts. BMC Genomics **11:**414. http://dx.doi.org/10.1186/1471-2164-11-414.
34. **Homann OR, Johnson AD.** 2010. MochiView: versatile software for genome browsing and DNA motif analysis. BMC Biol. **8:**49. http://dx.doi.org/10.1186/1741-7007-8-49.
35. **Machanick P, Bailey TL.** 2011. MEME-ChIP: motif analysis of large DNA datasets. Bioinformatics **27:**1696–1697. http://dx.doi.org/10.1093/bioinformatics/btr189.